



Original Article

Mesenchymal stem cells cultured under hypoxic conditions had a greater therapeutic effect on mice with liver cirrhosis compared to those cultured under normal oxygen conditions

Yuichi Kojima^a, Atsunori Tsuchiya^{a,*}, Masahiro Ogawa^a, Shunsuke Nojiri^a,
Suguru Takeuchi^a, Takayuki Watanabe^a, Kenji Nakajima^b, Yukio Hara^b,
Junji Yamashita^b, Junichi Kikuta^c, Masaaki Takamura^a, Masaru Ishii^c, Shuji Terai^{a,**}

^a Division of Gastroenterology and Hepatology, Graduate School of Medical and Dental Sciences, Niigata University, 1-757 Asahimachi-dori, Chuo-ku, Niigata, 951-8510, Japan

^b Research Laboratory, Nihon Pharmaceutical Co Ltd, 34 Shin-izumi, Narita-City, Chiba, 286-0825, Japan

^c Department of Immunology and Cell Biology, Graduate School of Medicine and Frontier Biosciences, Osaka University, 2-2 Yamada-oka, Suita, Osaka, 565-0871, Japan

ARTICLE INFO

Article history:

Received 3 July 2019

Received in revised form

18 August 2019

Accepted 29 August 2019

Keywords:

Mesenchymal stem cells

Hypoxic condition

Liver cirrhosis

PGE2

miR210

ABSTRACT

Background: Mesenchymal stem cells (MSCs) can be easily expanded. They can be acquired from medical waste such as adipose and umbilical cord tissues, are influenced by culturing conditions, and exert anti-inflammatory, antioxidant, anti-fibrotic, and angiogenic effects. We analyzed the multi-directional effects of MSCs cultured under hypoxic conditions and their underlying mechanisms in the treatment of liver cirrhosis in a mouse model.

Methods: Human bone marrow-derived MSCs cultured under hypoxic (5% O₂; hypoMSCs) and normoxic (21% O₂; norMSCs) conditions were compared by cap analysis of gene expression (CAGE) with or without serum from liver cirrhosis patients. The therapeutic effects of MSCs, including serum liver enzyme induction, fibrosis regression, and hepatic oxidative stress, were evaluated by injecting 1×10^6 , 2×10^5 , or 4×10^4 MSCs/mouse into the tail veins of mice with carbon tetrachloride (CCl₄)-induced liver cirrhosis. Intravital imaging was performed with a two-photon excitation microscope to confirm the various MSC migration paths to the liver.

Results: CAGE analysis revealed that the RNA expression levels of prostaglandin E synthase (*Ptges*) and miR210 were significantly higher in hypoMSCs than in norMSCs. *In vivo* analysis revealed that both hypoMSCs and norMSCs reduced serum alanine aminotransferase, oxidative stress, and fibrosis compared to that in control mice in a dose-dependent manner. However, hypoMSCs had stronger therapeutic effects than norMSCs. We confirmed this observation by an *in vitro* study in which hypoMSCs changed macrophage polarity to an anti-inflammatory phenotype via prostaglandin E2 (PGE2) stimulation. In addition, miR210 reduced the rate of hepatocyte apoptosis. Intravital imaging after MSC administration showed that both cell types were primarily trapped in the lungs. Relatively a few hypoMSCs and norMSCs migrated to the liver. There were no significant differences in their distributions.

Conclusion: The therapeutic effect of hypoMSCs was mediated by PGE2 and miR210 production and was greater than that of norMSCs. Therefore, MSCs can be manipulated to improve their therapeutic efficacy

Abbreviations: MSCs, Mesenchymal stem cells; norMSCs, MSCs cultured under normal oxygen (21% O₂) conditions; hypoMSCs, MSCs cultured under hypoxic oxygen (5% O₂) conditions; CAGE, Cap analysis of gene expression; id-BMM, Induced Bone Marrow Derived Macrophage; HHStc, Human Hepatic Stellate Cells; LC, Liver cirrhosis; NASH, Non-alcoholic steatohepatitis; CCl₄, Carbon tetrachloride; ALT, Alanine aminotransferase; ALP, Alkaline phosphatase; T-Bil, Total bilirubin; ALB, Albumin; SOD, Superoxide dismutase; MDA, Malondialdehyde; 8-OHdG, DNA 8-hydroxy-2'-deoxyguanosine; ECM, Extracellular matrix; LPS, Lipopolysaccharide; PGE2, Prostaglandin E2; PCR, Polymerase chain reaction.

* Corresponding author. Niigata University, 1-757 Asahimachi-dori, Chuo-ku, Niigata, 951-8510, Japan. Fax: +81 25 227 0776.

** Corresponding author.

E-mail addresses: y-kojima@med.niigata-u.ac.jp (Y. Kojima), atsunori@med.niigata-u.ac.jp (A. Tsuchiya), shigusawakino@yahoo.co.jp (M. Ogawa), nojiri.joetsu@gmail.com (S. Nojiri), sugu01@med.niigata-u.ac.jp (S. Takeuchi), watanabe-ta@med.niigata-u.ac.jp (T. Watanabe), knakajima@nihon-pharm.co.jp (K. Nakajima), y.hara@nihon-pharm.co.jp (Y. Hara), j.yamashita@nihon-pharm.co.jp (J. Yamashita), jikikuta@icb.med.osaka-u.ac.jp (J. Kikuta), atmc@med.niigata-u.ac.jp (M. Takamura), mishii@icb.med.osaka-u.ac.jp (M. Ishii), terais@med.niigata-u.ac.jp (S. Terai).

Peer review under responsibility of the Japanese Society for Regenerative Medicine.

<https://doi.org/10.1016/j.reth.2019.08.005>

2352-3204/© 2019, The Japanese Society for Regenerative Medicine. Production and hosting by Elsevier B.V. This is an open access article under the CC BY-NC-ND license (<http://creativecommons.org/licenses/by-nc-nd/4.0/>).

in the treatment of liver cirrhosis and could potentially serve in effective cell therapy. MSCs produce several factors with multidirectional effects and function as “conducting cells” in liver cirrhosis.

© 2019, The Japanese Society for Regenerative Medicine. Production and hosting by Elsevier B.V. This is an open access article under the CC BY-NC-ND license (<http://creativecommons.org/licenses/by-nc-nd/4.0/>).

1. Background

Chronic liver damage is caused mainly by hepatitis B and C viruses and alcoholic- and non-alcoholic steatohepatitis (NASH). These conditions can induce liver fibrosis and, in some cases, liver cirrhosis. This disorder is frequently associated with liver dysfunction and may lead to port-systemic shunts and hepatocellular carcinoma. Decompensated liver cirrhosis is a life-threatening disease [1]. The prognosis of progressive liver cirrhosis—such as those classified as Child-Pugh grades B and C—is poor, and liver transplantation is the only effective treatment. However, there is a chronic shortage of donor organs. For this reason, a new therapy is needed to regress fibrosis and improve liver function. Liver disease regression can be accomplished by the effective treatment and control of its causes. Previous reports have indicated that liver fibrosis regressed after treating hepatitis C with direct-acting antivirals [2,3] and by treating hepatitis B with a nucleotide analog [4]. Therefore, humans can regress liver fibrosis, and the effective induction of this ability may be an ideal liver cirrhosis treatment. Liver fibrosis can lead to the following extracellular matrix (ECM)-related disorders: hepatocyte injury, inflammation, myofibroblast activation, and the dysregulated production of ECM components [5]. Drugs targeting this fibrogenesis cascade may potentially serve as novel strategies. Although some of these are being evaluated in clinical studies, none of them have yet been approved to test their effects on liver fibrosis regression.

Several clinical trials on cell therapies targeting fibrosis regression are underway. The most popular are those involving mesenchymal stem cells (MSCs) [6,7]. MSCs are obtained from the bone marrow, adipose tissues, umbilical cord tissues, and dental pulp. They readily expand and differentiate into osteoblasts, adipocytes, and chondrocytes after induction. MSCs are a heterogeneous population presenting species-specific surface markers such as CD105 and CD73. Previous intravital imaging studies using two-photon excitation microscopy showed that most MSCs injected into the mouse tail vein were trapped in the lungs, and only a few migrated to the liver. In a liver cirrhosis model, they disappeared from the liver, lung, and spleen after 7 d [8]. MSCs secrete various cytokines, chemokines, growth factors, and exosomes that affect immune cells including macrophages, T cells, and B cells. They indirectly and remotely affect tissue repair by functioning as “conducting cells.” Depending on the host condition, MSCs regulate trophic factors and indirectly mediate anti-apoptotic, antioxidant, antifibrotic, angiogenic, and immunosuppressive effects. Since they have multiple functions, readily expand, and are minimally antigenic, both autologous and allogeneic MSCs have been used in >900 clinical trials to treat various diseases. Several basic studies have been conducted using MSCs to treat various liver disease models such as cirrhosis, NASH, and acute injury. To date, ~50 trials have used autologous and allogeneic MSCs to target acute and chronic liver diseases. The cells were administered by injection into the peripheral vein, hepatic artery, or portal vein [9].

The origins, culture conditions, and effective administration routes of MSCs have not yet been optimized. In the present study, we investigated the effects of low-oxygen preconditioning on MSC efficacy in the treatment of a mouse liver cirrhosis model. We

evaluated the changes in MSC properties resulting from hypoxia induction and the addition of human patient serum, and confirmed them via Cap Analysis Gene Expression (CAGE). It was determined that several MSC factors were upregulated in response to hypoxia.

2. Methods

2.1. Preparation of MSCs

Poietics human MSCs (passage 2) were purchased from Lonza (Basel, Switzerland), expanded until passage 4, and used as normoxic MSCs (norMSCs). The cells were cultured and passaged with StemPro MSC SFM XenoFree (Thermo Fisher Scientific, Waltham, MA, USA) under normal oxygen conditions (21% O₂) and 5% CO₂ at 37 °C. Passage 4 cells were frozen and stored using liquid nitrogen. StemPro BM MSCs (passage 4; Thermo Fisher Scientific) were purchased from Thermo Fisher Scientific and used as hypoxic MSCs (hypoMSCs). The cells were cultured in StemPro MSC SFM XenoFree (Thermo Fisher Scientific) under hypoxic conditions (5% O₂) and 5% CO₂ at 37 °C. Cryopreservation solution with 10% DMSO was used for cryopreservation of these cells.

2.2. CAGE analysis

Serum was obtained from three liver cirrhosis patients (Table 1) and one healthy person. All experiments were approved by the Ethics Committee of Niigata University, Niigata, Japan. The mRNAs from MSCs grown for 48 h with or without serum were analyzed by CAGE (K.K. DNAFORM, Yokohama, Japan).

2.3. Induced bone marrow-derived macrophage (id-BMM) preparation

Ten- to 12-week-old male C57BL/6 mice were sacrificed by cervical dislocation and their limbs were removed. Bone marrow precursors were flushed from the medullary cavities of the tibias and femurs using DMEM (Thermo Fisher Scientific) with a 25G needle. The id-BMMs were cultured at 37 °C under 5% CO₂ in ultra-low attachment flasks (Corning, Armonk, NY, USA) containing DMEM/F12 (Thermo Fisher Scientific) and 20 ng/mL macrophage colony-stimulating factor (M-CSF; CSF-1; recombinant murine M-CSF; Peprotech Inc., Rocky Hill, NJ, USA). The id-BMMs were cultured for 7 d and the medium was replaced twice weekly.

2.4. Co-culture of id-BMMs and norMSCs or hypoMSCs

The id-BMMs were cultured with or without MSCs at 37 °C under 5% CO₂ in Transwell 6-well plates (Corning) for 72 h. The id-BMMs were then harvested and their tumor necrosis factor- α (*Tnf α*), *Ym-1*, *Fizz-1*, *Cd206*, and *MCP-1* mRNA levels were compared to those of the controls. Prostaglandin E synthase (*Ptges*) from hypoMSCs was knocked down with HiPerFect Transfection Reagent (Qiagen, Hilden, Germany) according to the manufacturer's instructions. Macrophages were cultured either with hypoMSCs or *Ptges*-knockdown hypoMSCs and the mRNA expression levels of their polarization-related markers were compared.

Table 1
Information of the three liver cirrhosis patients.

	sex	age	etiology	Child-Pugh Score	ALT (U/l)	Platelets (× 10000/μl)
LC1	F	54	Alcohol	B (8)	14	5.7
LC2	M	67	Alcohol	A (5)	22	13.6
LC3	F	80	NASH	B (7)	20	6.1

ALT: alanine aminotransferase, NASH: non-alcoholic steatohepatitis.

2.5. Mice

Eight-week-old C57BL/6 male mice were purchased from Charles River (Yokohama, Japan). They were housed in a pathogen-free environment and kept under standard laboratory conditions with a 12-h day/night cycle and access to food and water *ad libitum*. All animal experiments were in compliance with the regulations of and approved by the Institutional Animal Care and Committee at Niigata and Osaka Universities.

2.6. Preparation of the cirrhosis mouse model and cell transplantation

Male mice were intraperitoneally injected with 1.0 mL/kg carbon tetrachloride (CCl₄; Wako Pure Chemical Industries Ltd.) to induce cirrhosis. CCl₄ was dissolved in corn oil (Wako Pure Chemical Industries Ltd.) at a 1:10 volumetric ratio. The mice received CCl₄ i.p. twice weekly over a 12-week period. They were then randomly assigned to one of eight groups: CCl₄ + PBS (control); CCl₄ + 1 × 10⁶ norMSCs or hypoMSCs; CCl₄ + 2 × 10⁵ norMSCs or hypoMSCs; and CCl₄ + 4 × 10⁴ norMSCs or hypoMSCs. Mice not subjected to CCl₄ treatment served as a normal control. At eight weeks, either PBS or one of the aforementioned cell types was injected into CCl₄-induced mice through the tail vein without immunosuppressive agents. The mice were euthanized at four weeks after cell injection.

2.7. Biochemical analysis

Blood samples were taken from the abdominal aortas of the mice at four weeks after cell injection. Serum was also collected. Serum alanine aminotransferase (ALT), alkaline phosphatase (ALP), total bilirubin (T-BIL), and albumin (ALB) concentrations were determined by BML Inc. (Tokyo, Japan).

2.8. Oxidative stress analysis

Liver tissue was excised from the mice at 7 d and 28 d after treatment. The levels of superoxide dismutase (SOD), total glutathione, DNA 8-hydroxy-2'-deoxyguanosine (8-OHdG), and malondialdehyde (MDA) in the liver tissue were measured as oxidative stress markers. SOD was measured using the SOD Assay kit–WST (Dojindo, Kumamoto, Japan), total glutathione was measured with a GSSG/GSH Quantification kit (Dojindo), 8-OHdG was measured with a High Sensitive 8-OHdG Check ELISA kit (JalCA, Shizuoka, Japan), and MDA was measured with a lipid peroxidation (MDA) assay kit (Abcam, Cambridge, England). All tests were conducted according to the manufacturer's instructions.

2.9. Histopathological analysis

Liver tissue was excised, fixed in 10% formalin, embedded in paraffin wax, and sliced into 4-μm sections. The paraffin sections were deparaffinized, rehydrated, and stained with hematoxylin and

eosin (H&E) and Sirius red for histological examination following the manufacturer's standard protocols. Photographs were taken from randomly chosen sections using the HS all-in-one fluorescence microscope (BZ-9000; Keyence, Osaka, Japan). A quantitative analysis of fifty randomly selected fibrotic areas was performed using ImageJ v. 1.6.0.20 (NIH, Bethesda, MD, USA).

2.10. Hydroxyproline assay

The liver cirrhosis mouse model at 4 weeks after cell administration was used to determine the levels of hydroxyproline, which is a representative collagen component. Liver samples (20 mg) were homogenized and subjected to a QuickZyme Hydroxyproline Assay (QuickZyme Bioscience, Zernikedreef, Netherland) according to the manufacturer's protocol. Samples were extracted and their absorbances were measured at 570 nm. Data were expressed as the weight of hydroxyproline in 1 mg liver tissue.

2.11. In vivo imaging

HypoMSCs were stained green with a Green Fluorescent Cell Linker kit (Sigma Aldrich, St. Louis, MO, USA). NorMSCs were stained red with a Red Fluorescent Cell Linker kit (Sigma Aldrich). Staining was done according to the manufacturer's instructions. Then, 5 × 10⁵ cells from each type of MSCs were injected into the cirrhosis model mice through the tail vein. Six hours after treatment, the mice were anesthetized with isoflurane and the median lobes of their livers were surgically exposed. Their internal liver surfaces were observed under an imaging system consisting of a two-photon inverted microscope (A1R-MP, Nikon, Tokyo, Japan) driven by a laser (Chameleon Vision Ti: Sapphire, Coherent) tuned to 880 nm and fitted with a water multi-immersion objective lens (Plan Fluor; N.A., 0.75; Nikon, Tokyo, Japan). Raw imaging data were processed with Imaris (Bitplane, Zurich, Switzerland).

2.12. Real-time PCR

Total RNA was reverse-transcribed with a QuantiTect reverse transcription kit (Qiagen). Gene expression was analyzed using pre-validated QuantiTect primers (Supplemental Table 1) and QuantiTect SYBR reagent (Qiagen, Hilden, Germany). Real-time PCR was conducted with a Step One Plus Real-time PCR System (Applied Biosystems, Foster City, CA, USA). The results were derived from ≥3 separate samples. *GAPDH* was used as an internal control. The fold change in gene expression relative to the control was calculated by the 2^{-ΔΔCt} method.

2.13. Hepatocyte and human hepatic stellate cell apoptosis

PXB cells (fresh hepatocytes) were purchased from PhoenixBio (Hiroshima, Japan) and cultured on a 96-well plate according to the manufacturer's instructions. Human Hepatic Stellate Cells (HHStEC) were purchased from ScienCell Research Laboratories (Carlsbad, CA, USA) and cultured on a 96-well plate according to the

manufacturer's instructions. PXB and HHStc cells were transfected with lipofectamine, miR210 mimic, or miRNA210 inhibitor using Lipofectamine RNAiMAX Transfection Reagent (Thermo Fisher Scientific). Apoptosis was induced by adding 1000-fold diluted actinomycin D to the medium. Twelve hours after treatment, the cells were treated with an Apoptotic/Necrotic Cells Detection Kit (PromoCell, Heidelberg, Germany) according to the manufacturer's instructions and observed under a fluorescence microscope.

2.14. Statistical analysis

Data were processed in GraphPad Prism v. 7 (GraphPad Software Inc., La Jolla, CA, USA) and are presented as means \pm SD. All data were normally distributed. The results were assessed by Student's *t*-test. Differences between groups were analyzed by one-way ANOVA and were considered significantly different at $P < 0.05$.

3. Results

3.1. HypoMSCs produced more PTGES and miR-210 than norMSCs

CAGE was used to compare the mRNA levels of hypoMSCs and norMSCs in the absence of human serum or in the presence of serum derived from a healthy individual or a liver cirrhosis (LC) patient. Sera derived from healthy individuals or those with LC were used to analyze the effects of humoral factors in serum. A heat map (Fig. 1A) revealed that without human serum, the mRNA expression patterns of hypoMSCs and norMSCs markedly differed. In contrast, the differences in mRNA expression were comparatively small between MSCs (both hypoMSCs and norMSCs) grown with serum from a healthy person and those grown with serum from LC patients.

Global gene expression patterns were compared between hypoMSCs and norMSCs cultured with or without human serum. We selected RNAs whose expression levels were $>4 \times$ higher in hypoMSCs than in norMSCs. The miR210, *Ptges*, *Il-6*, and *Cxcl1*, 2, 3, and 6 were substantially upregulated in hypoMSCs relative to norMSCs. Moreover, after adding normal or LC human serum to both MSCs, *Aldh*, *Il-8*, and *Hgf* were considerably upregulated in hypoMSCs compared to norMSCs.

3.2. HypoMSCs decreased liver damage and fibrosis in mice in a dose-dependent manner

To investigate the therapeutic effect of hypoMSCs, hypo- and norMSCs were administered to CCl₄-induced liver cirrhosis mice at 1×10^6 cells/mouse, 2×10^5 cells/mouse, and 4×10^4 cells/mouse (Fig. 2A). Four weeks after the injections, the serum ALT levels in the hypoMSC groups were 104.2 ± 7.0 U/L (1×10^6 cells/mouse), 126.8 ± 15.5 U/L (2×10^5 cells/mouse), and 149.1 ± 26.9 U/L (4×10^4 cells/mouse). In the norMSC groups, they were 114.9 ± 16.3 U/L (1×10^6 cells/mouse), 155.8 ± 26.8 U/L (2×10^5 cells/mouse), and 206.2 ± 30.8 U/L (4×10^4 cells/mouse). Therefore, serum ALT was suppressed in a dose-dependent manner. However, hypoMSCs tended to have lower serum ALT levels than norMSCs (Fig. 2B).

We evaluated liver fibrosis using Sirius red staining and hydroxyproline quantitation. The areas stained with Sirius red in the hypoMSC groups made up $4.4 \pm 0.1\%$ (1×10^6 cells/mouse), $4.6 \pm 0.1\%$ (2×10^5 cells/mouse), and $4.8 \pm 0.1\%$ (4×10^4 cells/mouse) of the total area. For the norMSC groups, $4.7 \pm 0.2\%$ (1×10^6 cells/mouse), $4.9 \pm 0.2\%$ (2×10^5 cells/mouse), and $5.2 \pm 0.2\%$ (4×10^4 cells/mouse) of the total areas were stained (Fig. 3A and B). The hydroxyproline levels in the hypoMSC groups were 1.2 ± 0.04 μ M/mg liver (1×10^6 cells/mouse), 1.2 ± 0.03 μ M/mg liver (2×10^5 cells/mouse), and 1.3 ± 0.05 μ M/mg liver

(4×10^4 cells/mouse). For the norMSC groups, they were 1.3 ± 0.04 μ M/mg liver (1×10^6 cells/mouse), 1.5 ± 0.14 μ M/mg liver (2×10^5 cells/mouse), and 1.7 ± 0.12 μ M/mg liver (4×10^4 cells/mouse). Therefore, liver fibrosis was improved in a dose-dependent manner by all treatments. Nevertheless, hypoMSCs were more effective at mitigating liver fibrosis than norMSCs (Fig. 3C). Overall, hypoMSCs decreased liver damage and fibrosis in the mice in a dose-dependent manner.

3.3. HypoMSCs induced anti-inflammatory macrophage growth via prostaglandin E2 production

MSCs may affect macrophage polarity via several factors, including prostaglandin E2 (PGE2) [10]. According to our CAGE analysis, however, hypoMSCs expressed *Ptges* more strongly than norMSCs. In the present study, we compared macrophage polarization between hypoMSCs and norMSCs and determined whether the discrepancy between them could be explained by their relative differences in PGE2 expression.

Macrophages were cultured from bone marrow with M-CSF for 7 d. They were then incubated with either hypoMSCs or norMSCs and their mRNAs were compared to detect the expression of polarization-related markers. The anti-inflammatory marker *Cd206* was upregulated in both hypoMSC- and norMSC-treated macrophages, and the anti-inflammatory marker *Ym-1* was upregulated in hypoMSC-treated macrophages. In contrast, the pro-inflammatory markers *Tnf α* and *Mcp-1* were significantly downregulated in hypoMSC-treated macrophages compared to levels in norMSC-treated macrophages. Therefore, hypoMSCs tended to induce anti-inflammatory macrophages more strongly than norMSCs (Fig. 4A). We proposed that this discrepancy was caused by the relative differences in *Ptges* expression between hypoMSC- and norMSC-treated macrophages. To test this hypothesis, we knocked down *Ptges* in hypoMSCs with siRNA (Fig. 4B), incubated macrophages with either hypoMSCs or *Ptges*-knockdown hypoMSCs, and compared their mRNA expression levels of polarization-related markers (control; macrophages cultured without MSCs). We confirmed that *Cd206* and *Ym-1* were upregulated and that *Tnf α* was downregulated in macrophages grown with hypoMSCs. In macrophages cultured with *Ptges*-knockdown hypoMSCs, the expression levels of both *Cd206* and *Ym-1* tended to be lower, and that of *Tnf α* was significantly higher, than those in macrophages grown with normal hypoMSCs. Therefore, PGE partially influenced the anti-inflammatory phenotype of the macrophages (Fig. 4C).

3.4. HypoMSCs more effectively reduced oxidative stress than norMSCs in both the short- and long term

It was previously reported that MSCs reduce oxidative stress in the liver [11]. SOD, total glutathione, MDA, and 8-OHdG were measured in livers at days 7 (short-term) and 28 (long-term) after the injection of 1×10^6 hypoMSCs or norMSCs. Compared to a standardized control value of 1.0 ± 0.04 , the short-term SOD levels for the hypoMSC and norMSC groups were 0.8 ± 0.06 and 1.0 ± 0.1 , respectively. The short-term total glutathione levels for the control, hypoMSC, and norMSC groups were 86.9 ± 11.3 μ mol/L, 31.0 ± 5.4 μ mol/L, and 50.7 ± 4.1 μ mol/L, respectively. The short-term MDA levels for the control, hypoMSC, and norMSC groups were 0.1 ± 0.01 nmol/mg, 0.07 ± 0.01 nmol/mg, and 0.1 ± 0.01 nmol/mg, respectively. The short-term 8OHdG levels for the control, hypoMSC, and norMSC groups were 2.7 ± 0.02 ng/mL, 0.8 ± 0.1 ng/mL, and 2.0 ± 0.1 ng/mL, respectively. Therefore, oxidative stress was lower in the livers of mice receiving hypoMSC than in those receiving norMSC treatment (Fig. 5A). Compared to a

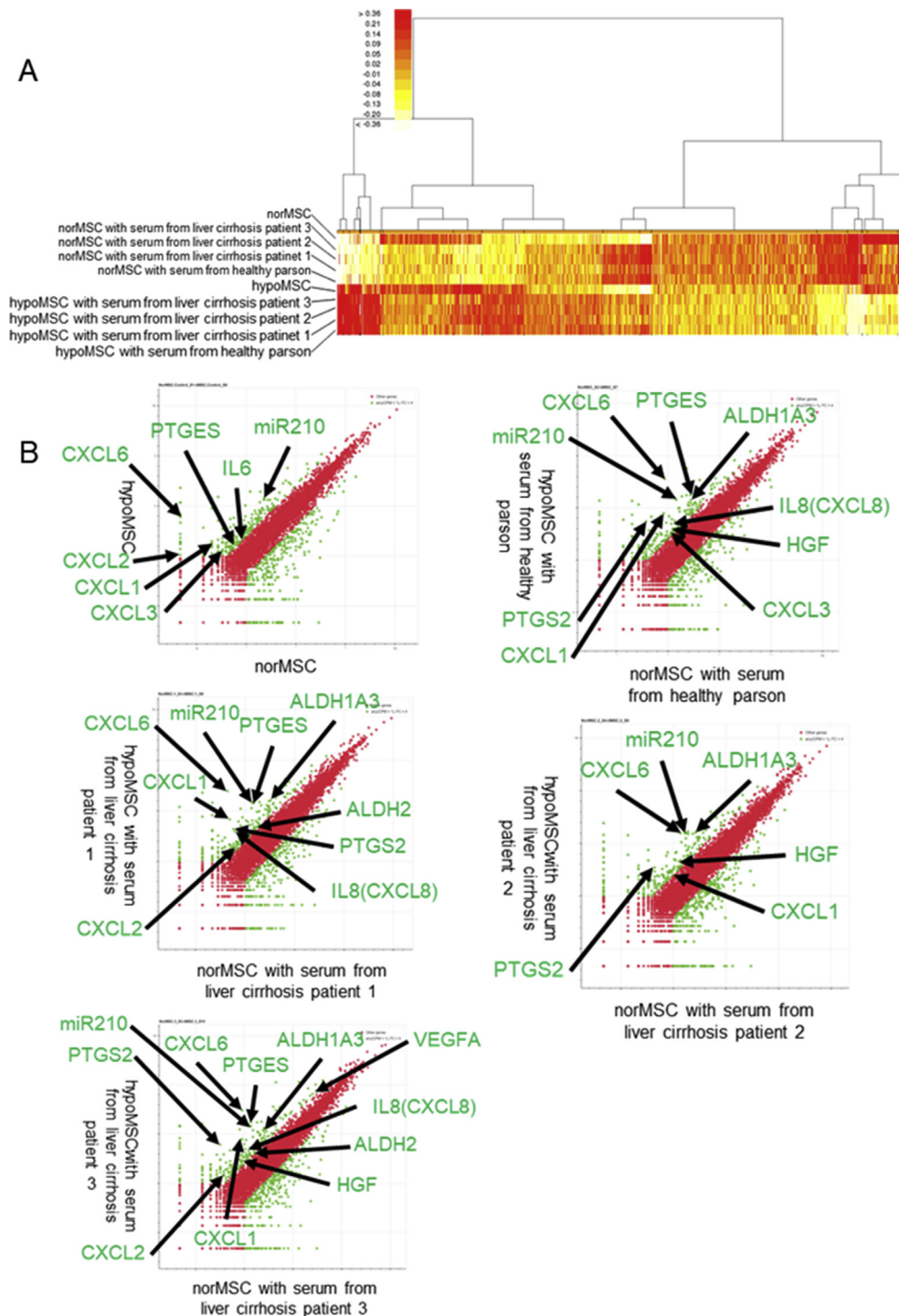


Fig. 1. Cap Analysis Gene Expression (CAGE) of mRNA expression changes in hypoxic MSCs (hypoMSCs) and normoxic MSCs (norMSCs) with or without serum from a healthy person or a liver cirrhosis (LC) patient. (A) A heat map revealed that the mRNA expression patterns of hypoMSCs and norMSCs markedly differed in the absence of human serum culture. Their mRNA expression levels changed after human serum was added. Relative differences in mRNA levels between MSCs cultured with healthy serum and those cultured with LC serum were smaller than those between MSCs cultured without human serum and those cultured with human serum. (B) The *miR210*, *Ptges*, *IL-6*, and *Cxcl1*, *2*, *3* and *6* genes were upregulated by $> 4 \times$ in hypoMSCs compared to those in norMSCs. After adding normal or LC serum to both MSCs, *Aldh*, *IL-8*, and *Hgf* were upregulated in hypoMSCs compared to that in norMSCs.

standardized control value of 1.0 ± 0.2 , the long-term SOD levels for the hypoMSC and norMSC groups were 0.5 ± 0.1 and 0.7 ± 0.1 , respectively. The long-term total glutathione levels for the control, hypoMSC, and norMSC groups were $78.9 \pm 5.5 \mu\text{mol/L}$, $29.4 \pm 3.0 \mu\text{mol/L}$, and $73.5 \pm 10.5 \mu\text{mol/L}$, respectively. The long-term MDA levels for the control, hypoMSC, and norMSC groups

were $0.7 \pm 0.1 \text{ nmol/mg}$, $0.5 \pm 0.02 \text{ nmol/mg}$, and $0.6 \pm 0.03 \text{ nmol/mg}$, respectively. The long-term 8OHdG levels for the control, hypoMSC, and norMSC groups were $3.7 \pm 0.4 \text{ ng/mL}$, $2.0 \pm 0.1 \text{ ng/mL}$, and $2.4 \pm 0.1 \text{ ng/mL}$, respectively. Therefore, the long-term oxidative stress levels were also lower in the livers of mice treated with hypoMSCs than they were in the those treated with

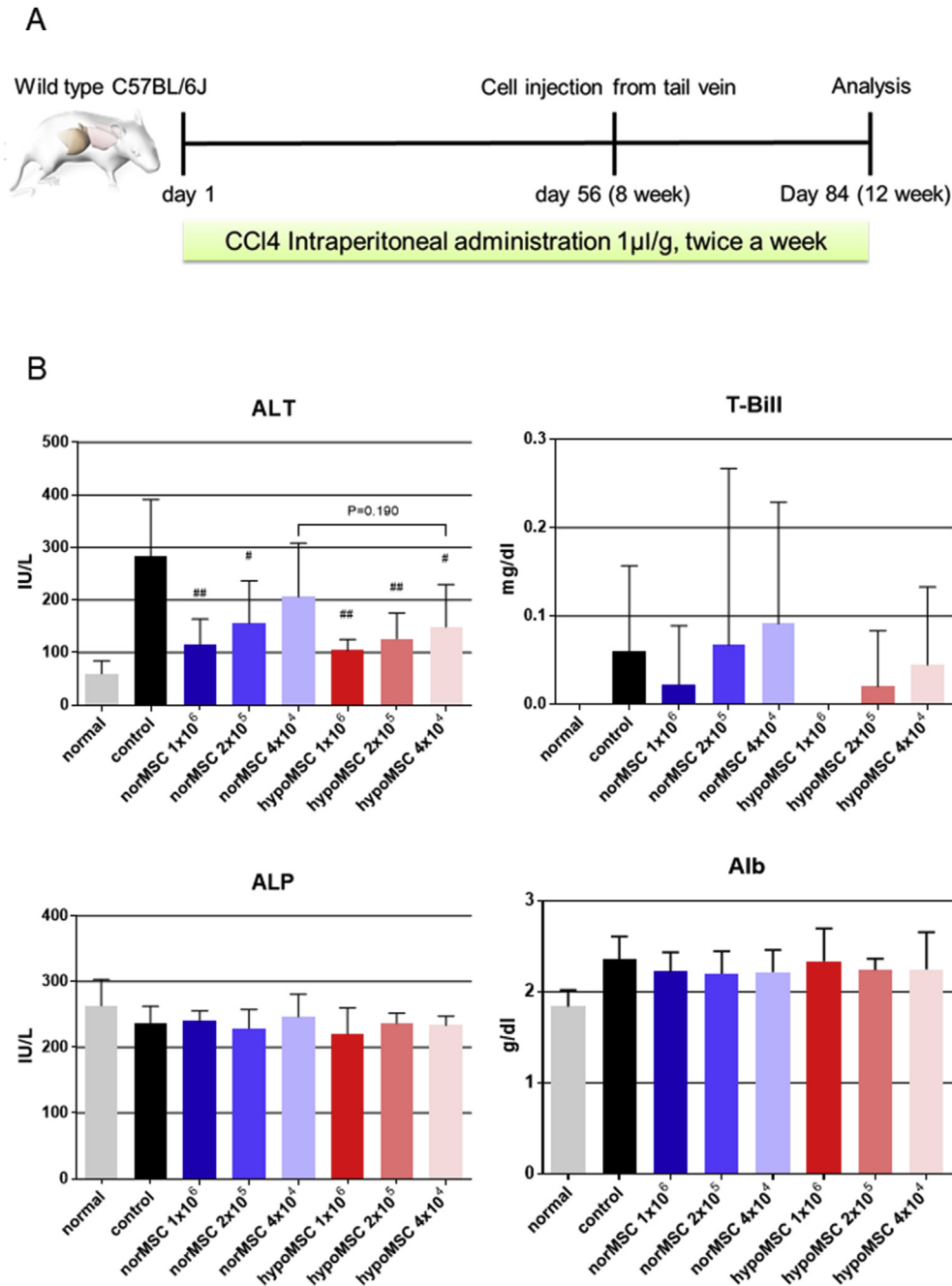


Fig. 2. Therapeutic effect of hypoMSCs and norMSCs on CCl₄-induced cirrhosis in mice. (A) Schematic diagram showing the fibrosis induction, cell administration, and analysis used in the present study. (B) Serum ALT, ALP, total bilirubin, and albumin levels four weeks after cell injection. Data are shown as means \pm SD; $n = 9$ –11 mice per group; $P < 0.001$ (ALT, hypoMSCs 1×10^6); $P < 0.001$ (ALT, hypoMSCs 2×10^5); $P < 0.01$ (ALT, hypoMSCs 4×10^4); $P < 0.001$ (ALT, norMSCs 1×10^6); $P < 0.01$ (ALT, norMSCs 2×10^5) relative to the control.

norMSCs (Fig. 5B). HypoMSCs more effectively reduced oxidative stress than norMSCs in both the short- and long-term treatments.

3.5. miR-210 reduced hepatocyte apoptosis

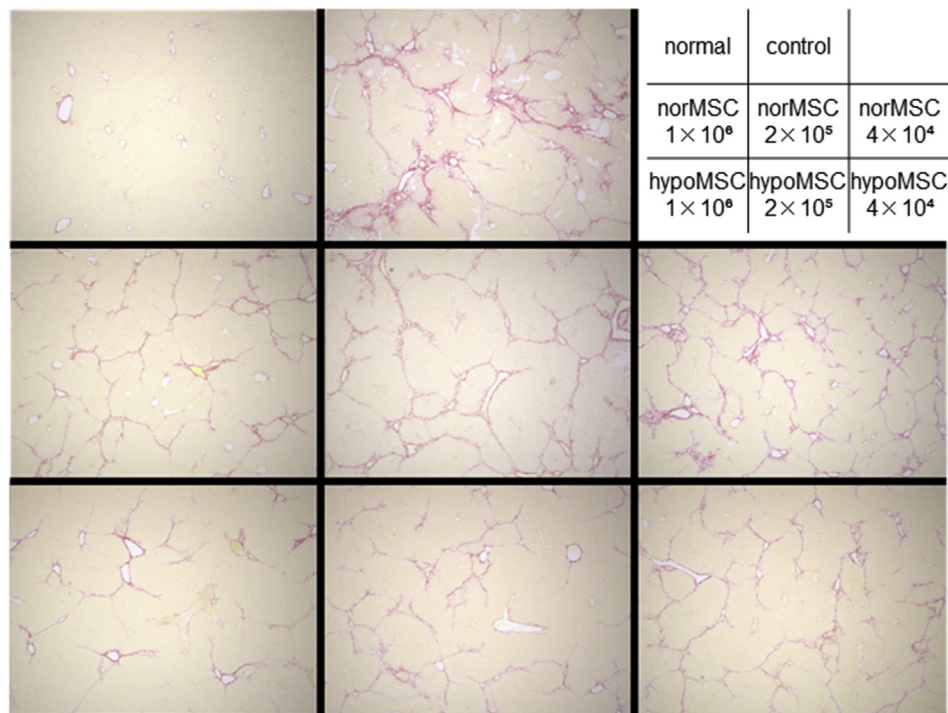
It was previously reported that miR-210 may reduce apoptosis in hepatic stellate cells and hepatocytes [12]. PXB cells (hepatocytes) and HHStcC were transfected with controls, miR-210 mimics, or miR-210 inhibitors. Apoptosis was then induced in the cells with actinomycin D and the proportion of apoptotic cells was enumerated. Apoptosis was not significantly reduced in HHStcC cells (control [lipofectamine]: $13.9 \pm 0.8\%$; miR-210 inhibitor:

$12.2 \pm 1.2\%$; miR-210 mimic: $14.1 \pm 0.9\%$) (Fig. 6A and C). However, apoptosis was significantly reduced in PXB cells (control [lipofectamine]: $9.5 \pm 0.3\%$; miR-210 inhibitor: $10.9 \pm 0.7\%$; miR-210 mimic: $7.8 \pm 0.7\%$) (Fig. 6B and D). Therefore, hypoMSCs reduced apoptosis in hepatocytes via miR-210.

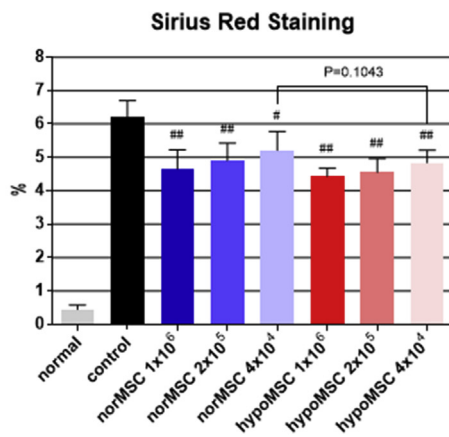
3.6. After injection, most norMSCs and hypoMSCs were trapped in the lungs and only a few migrated to the liver

We injected 5×10^5 red fluorescent norMSCs and 5×10^5 green fluorescent hypoMSCs into the tail veins of mice and tracked their movements and fate using a two-photon excitation microscope

A



B



C

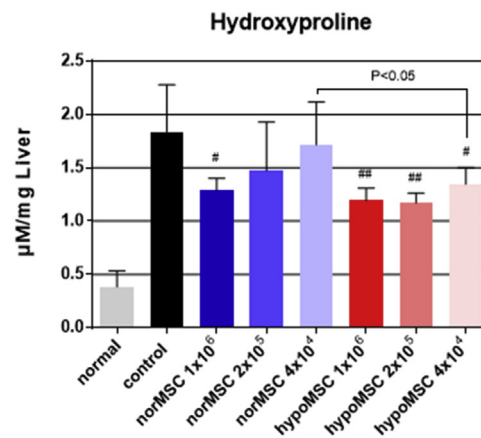


Fig. 3. Sirius red staining and hydroxyproline assay showing that hypoMSCs and norMSCs mitigated mouse liver fibrosis in a dose-dependent manner, but hypoMSCs decreased liver fibrosis more effectively than norMSCs. (A and B) Data are shown as means \pm SD; $n = 9-11$ mice per group; $P < 0.001$ (Sirius red, hypoMSCs 1×10^6 cells/mice); $P < 0.001$ (Sirius red, hypoMSCs 2×10^5 cells/mice); $P < 0.001$ (Sirius red, hypoMSCs 4×10^4 cells/mice); $P < 0.001$ (Sirius red, norMSCs 1×10^6 cells/mice); $P < 0.001$ (Sirius red, norMSCs 2×10^5 cells/mice); $P < 0.01$ (Sirius red, norMSCs 4×10^4 cells/mice) compared to the control. (C) Data are shown as means \pm SD; $n = 9-11$ mice per group; $P < 0.001$ (hydroxyproline, hypoMSCs 1×10^6 cells/mice); $P < 0.001$ (hydroxyproline, hypoMSCs 2×10^5 cells/mice); $P < 0.01$ (hydroxyproline, hypoMSCs 4×10^4 cells/mice); $P < 0.01$ (hydroxyproline, norMSCs 1×10^6 cells/mice) relative to the control.

(Fig. 7A). We monitored cell behavior in the liver, spleen, and lungs at 6 h after administration. Our findings corroborated those of our previous study, in which we used the same cirrhotic liver mouse model. The MSCs disappeared from the lung, liver, and spleen within 7 d. The cells migrating to the liver could be detected within 3 d, but especially on the day of injection. Most MSCs were trapped in the lungs, and only a very small proportion of both types of MSCs migrated to the liver. Therefore, humoral factors were found to

exhibit therapeutic effects (Fig. 7B). We could not distinguish between norMSCs and hypoMSCs among the cells that had migrated to the liver (Fig. 7C).

4. Discussion

Several clinical studies have reported on MSCs derived from different tissues, raised under various culture conditions, and used

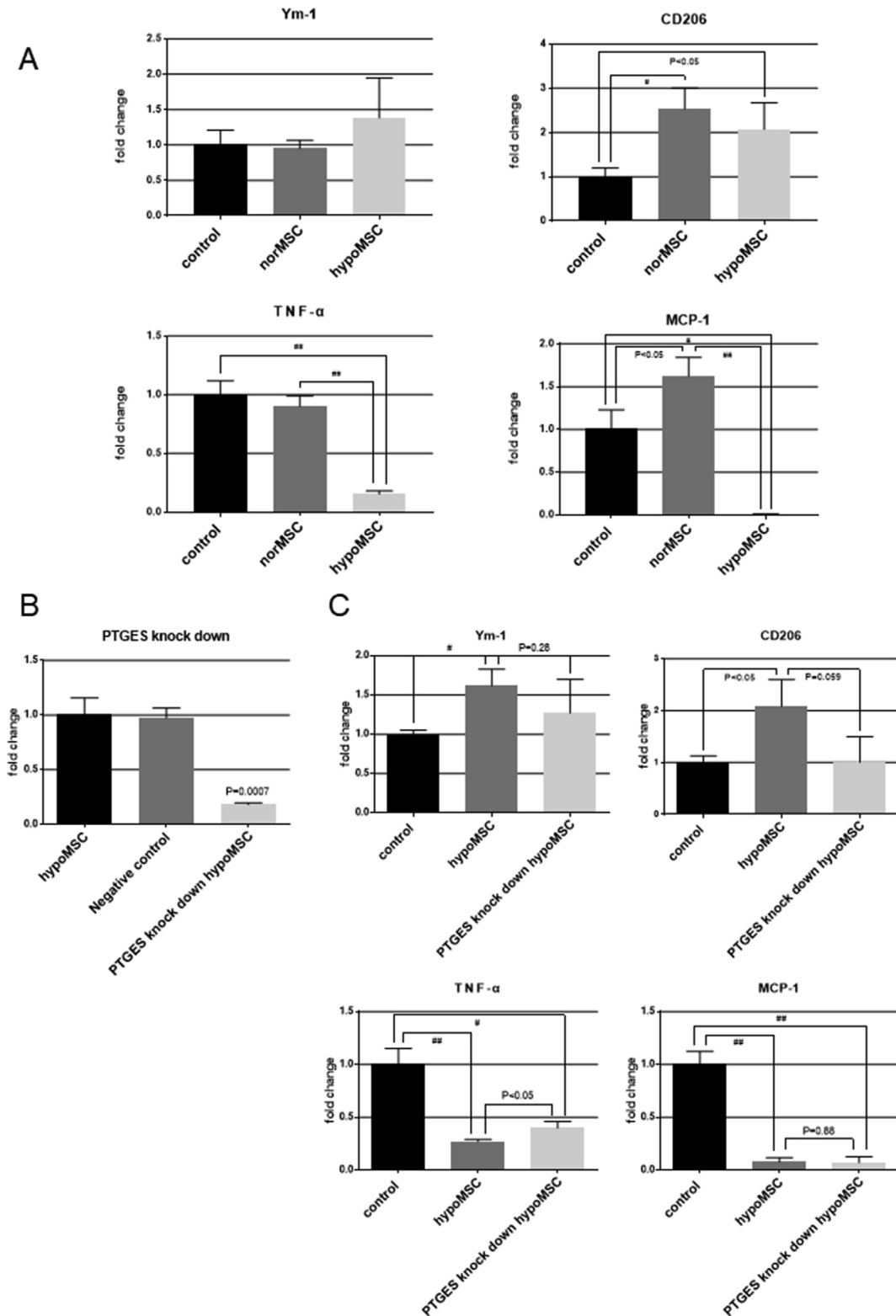


Fig. 4. HypoMSCs induced anti-inflammatory macrophages via prostaglandin E2 (PGE2) production. (A) mRNA expression changes in id-BMMs after co-culture with hypoMSCs or norMSCs. Anti-inflammatory marker *Cd206* ($P < 0.05$, hypoMSCs) ($P < 0.01$, norMSCs) levels were increased. Pro-inflammatory marker *Tnfα* ($P < 0.001$, hypoMSCs) and *Mcp-1* ($P < 0.01$, hypoMSCs) levels were decreased. (B) *Ptges* from hypoMSCs was knocked down with siRNA ($P = 0.0007$). (C) mRNA expression changes in id-BMMs after co-culture with hypoMSCs or *Ptges*-knockdown hypoMSCs. Levels of the anti-inflammatory markers *Cd206* ($P < 0.05$) and *Ym-1* ($P < 0.01$) increased and that of the pro-inflammatory marker *Tnfα* ($P < 0.001$) decreased in id-BMMs cultured with hypoMSCs. For macrophages cultured with *Ptges*-knockdown hypoMSCs, the expression levels of both *Cd206* and *Ym-1* were lower and that of *Tnfα* was higher ($P < 0.05$) than those in macrophages grown with normal hypoMSCs. Therefore, PGE influenced the anti-inflammatory phenotype of the macrophages.

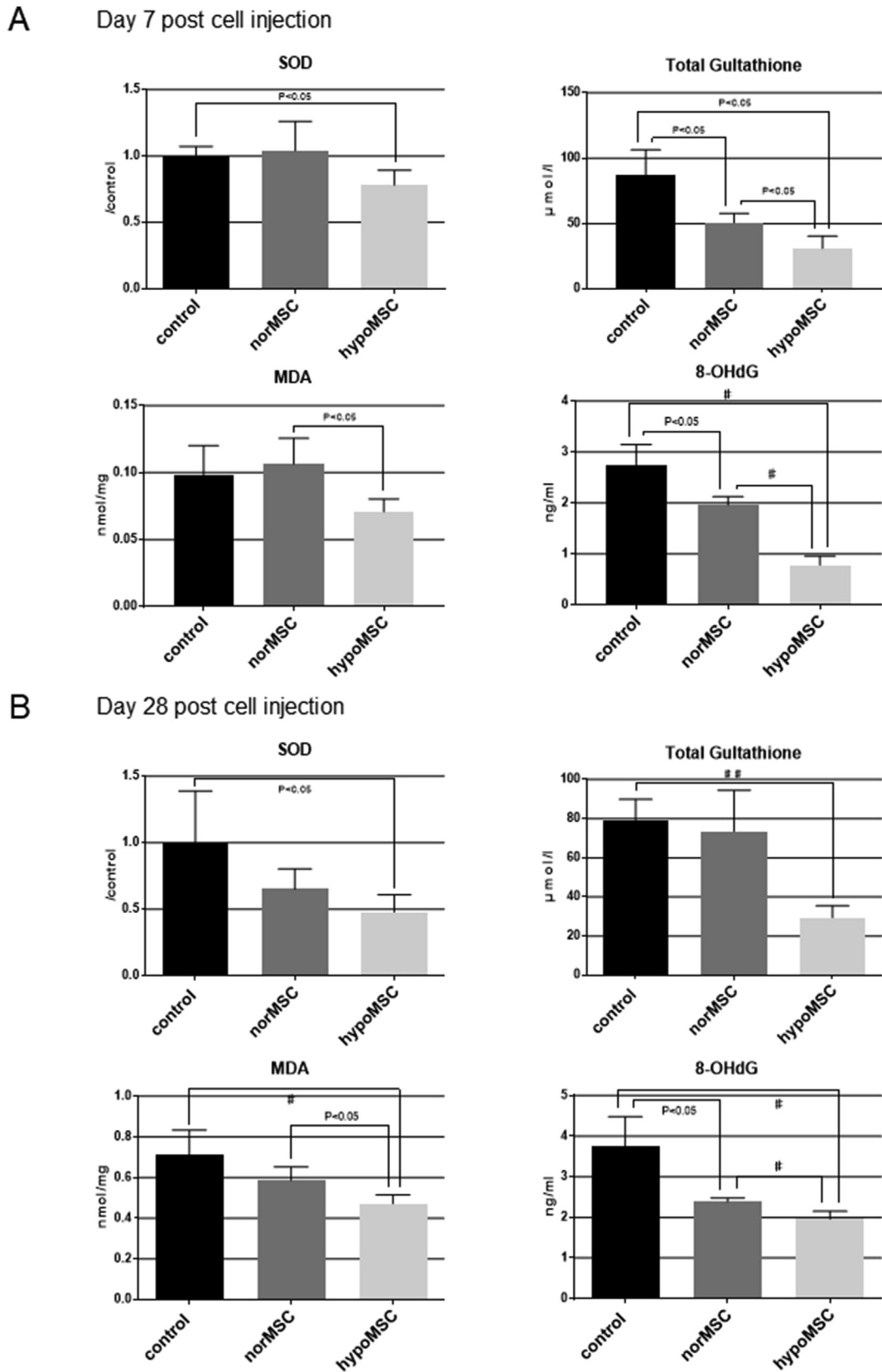


Fig. 5. Analysis of oxidative stress in the liver at 7 d and 28 d after cell administration. SOD, total glutathione, 8-OHdG, and MDA were measured as oxidative stress markers. (A) At day 7, SOD was reduced in the hypoMSC group ($P < 0.05$ compared to the control), total glutathione was reduced in the hypoMSC group ($P < 0.01$ compared to the control; $P < 0.05$ compared to norMSC), MDA was reduced in the hypoMSC group ($P < 0.05$ compared to norMSC), and 8-OHdG was reduced in the hypoMSC group ($P < 0.01$ compared to the control; $P < 0.01$ compared to norMSC). (B) By day 28, SOD was reduced in the hypoMSC group ($P < 0.05$ compared to the control), total glutathione was reduced in the hypoMSC group

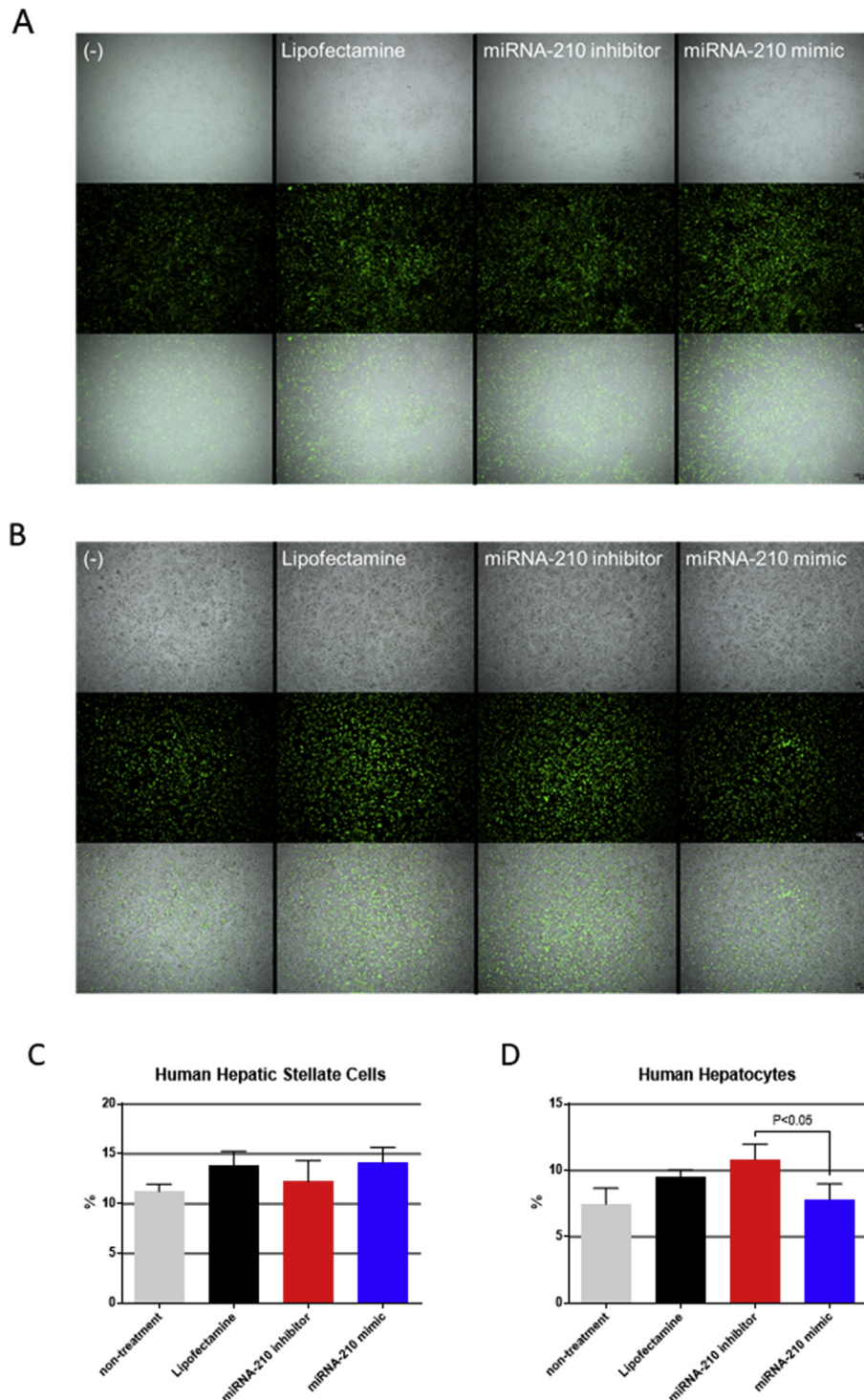


Fig. 6. miR-210 reduced apoptosis in hepatocytes but not human hepatic stellate cells (HHStec). (A and C) Apoptosis was not reduced in HHStec transfected with miR-210 mimic. (B and D) Apoptosis was reduced in hepatocytes transfected with miR-210 mimic ($P < 0.05$ compared to cells transfected with miR-210 inhibitor).

for the treatment of a number of diseases. However, the cell sources, culture conditions, and target diseases have not yet been optimized. In this study, we found that hypoMSCs were more efficacious than norMSCs for regressing fibrosis and decreasing oxidative stress in a CCl_4 -induced mouse liver cirrhosis model.

CAGE analysis indicated that PTGES and miR210 were upregulated in hypoMSCs relative to norMSCs. Our *in vitro* investigation showed that PTGES changed the macrophage phenotype to anti-inflammatory (M2), and that miR210 reduced hepatocyte apoptosis.

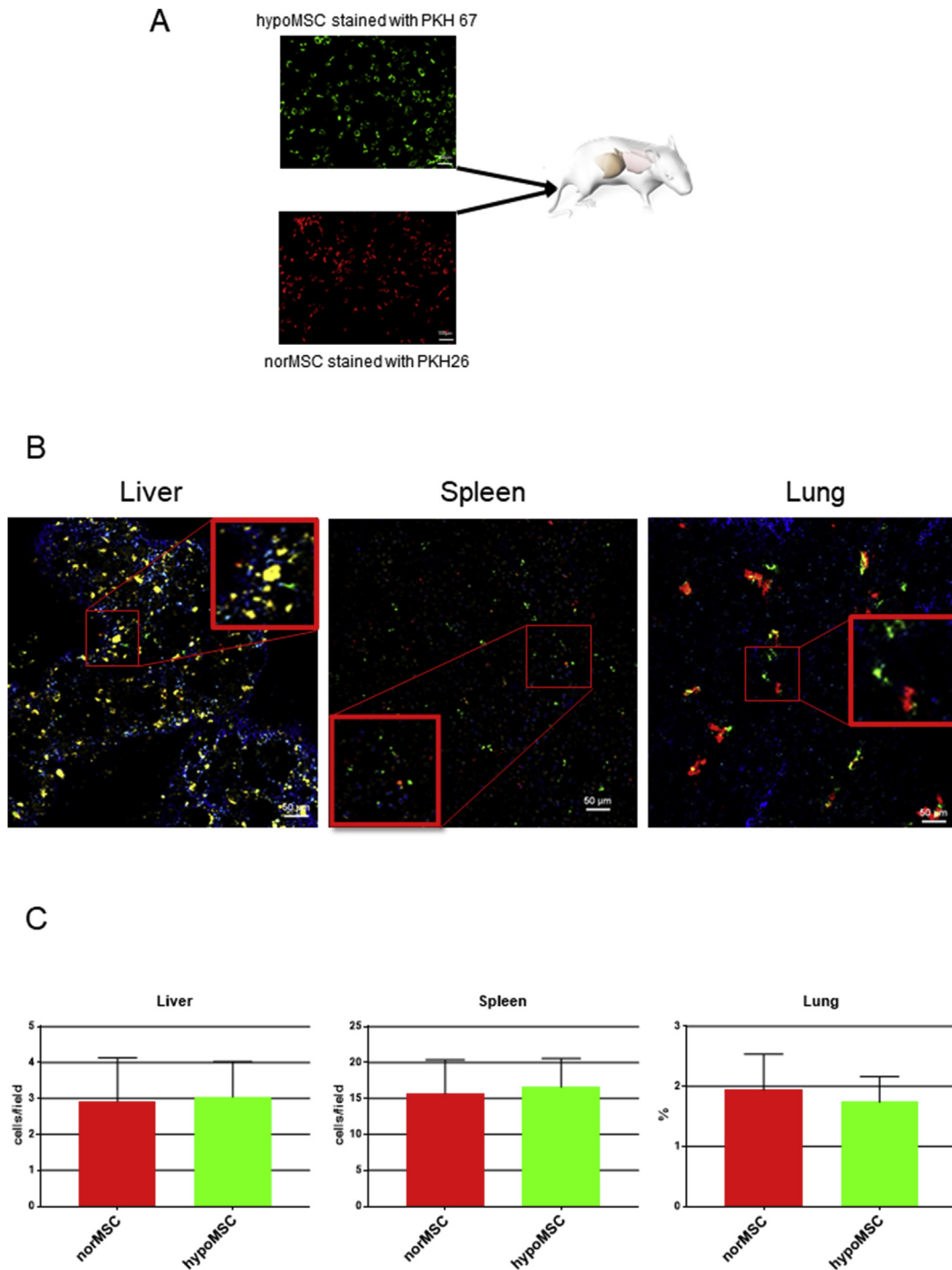


Fig. 7. Localization of hypoMSCs and norMSCs was assessed by intravital imaging analysis at 6 h after cell injection. (A) HypoMSCs and norMSCs were stained with green and red fluorescent dyes, respectively. Then, 5×10^5 cells from each MSC type were injected into a cirrhosis model mouse through the tail vein. (B) *In vivo* imaging of the liver (left panels), spleen (middle panels), and lung (right panels) was performed using a two-photon excitation microscope at 6 h after cell injection. Green, hypoMSCs. Red, norMSCs. Blue, collagen fibers (second harmonic generation). The dense blue fibrous area represents fibrosis. The yellow spots represent hepatocyte debris (scale bar: 50 μ m). (C) Distributions of the hypoMSCs and norMSCs in 50 random visual fields in the liver, spleen, and lung at 6 h after cell injection.

Previous studies reported that PGE2 was upregulated in MSCs preconditioned with lipopolysaccharide (LPS) plus TNF- α [10], or with interleukin-1 β (IL-1 β) plus interferon- γ (IFN- γ) [13]. In the present study, we found that hypoxia also induced PGE2 expression. Our results were consistent with previous studies reporting that direct PGE2 application in macrophages induced the M2-associated macrophage markers Arg1, IL-10, and matrix

metalloproteinase 9 (MMP9). Our previous paper confirmed that MSC-induced M2 polarization effectively regressed liver fibrosis and regenerated the liver [8]. A future objective is to customize MSC preconditioning for each specific target disease.

miR210 is a major hypoxia-inducible miR [12]. It plays several important roles in the antioxidant pathway, suppression of apoptosis, arrest of cell proliferation, repression of mitochondrial

respiration, interruption of DNA repair, and angiogenesis. It has been applied in cancer and stem cell research. In this study, we confirmed that miR210 is active against hepatocytes and stellate cells, and found that miR210 reduced hepatocyte apoptosis.

We also observed that the angiogenic factors IL-8 and ALDH were upregulated in hypoMSCs. Wang et al. reported that IL-8 secreted by human adipose-derived MSCs facilitated breast cancer growth by promoting angiogenesis [14]. Sherman et al. reported that MSCs with high aldehyde dehydrogenase activity had strong proliferative and vascular regenerative potential [15]. We proposed that both IL-8 and ALDH contributed to fibrosis regression and liver regeneration. Using transcriptome analysis, Elabd et al. indicated that the following factors were significantly upregulated in hypoMSCs compared to normMSCs: 1) inflammation modulation, C-X-C motif chemokine ligand 5 (CXCL5), and stromal cell derived factor 1 (SDF1); 2) cellular survival, migration, proliferation, glutathione peroxidase 3 (GPX3), LYL1 basic helix-loop-helix family member (LYL1), FES proto-oncogene, tyrosine kinase (FES), sperm-associated antigen 4 (SPAG4), transferrin receptor 2 (TR2), and thioredoxin interacting protein (TXNIP); 3) chondrolysis, cartilage metabolism; keratin 19 (KRT19), BARX homeobox 1 (BARX1), MyoD family inhibitor (MDF1), dachshund cadherin-related 1 (DCHS1); and 4) vasculogenesis and angiogenesis, desmin, ras-interacting protein 1 (RASIP1), LYL1, thioredoxin-interacting protein (TXNIP), and FES [16]. In the present study, the levels of SPAG4, BARX1, CKCL5, KRT19, and TXNIP were $>4 \times$, $>4 \times$, $>3.8 \times$, $>3.6 \times$, and $>2.5 \times$ higher, respectively, in hypoMSCs than in normMSCs.

Oxygen duration and concentration must be specified when inducing hypoxia. Burakova et al. reported that there are both short-term and permanent hypoxia exposure patterns. Short-term exposure is defined as within a duration of 72 h at an oxygen concentration of 0–5%. Permanent exposure is of a much longer duration at an oxygen level of 0–10%. While short-term exposure can cause both inhibitory and stimulatory effects, long-term culture may have several advantages over the former [17].

Gao et al. and other groups reported that MSC expansion is improved mainly by delaying senescence under low-oxygen conditions (0–7%), which also increase angiogenesis, anaerobic glycolysis, and ATP production [18]. Vertelov et al. reported that MSCs derived from human bone marrow presented with substantially higher targeted migration ability than normoxic cells, particularly in terms of wound healing-related factors such as members of the epidermal growth factor (EGF) family, the fibroblast growth factor family member vascular endothelial growth factor-121 (VEGF-121), platelet-derived growth factor-AB (PDGF-AB), IL-1 β , IL-6, and TNF- α [19]. They were also found to enhance the activation of hypoxia-inducible factor-1 (HIF-1) and Ras homolog A (RhoA) *in vitro* [19]. Yu et al. reported that hypoxia and low-dose induction of inflammation by TNF- α and IL-1 β synergistically enhanced bone marrow-derived MSC migration [20]. In the present study, HIF-1 α in hypoMSCs was slightly upregulated, the number of MSCs migrating to the liver did not markedly increase within 24 h, and only a few cells migrated to the liver. The target organ specificity of various MSCs with different tissue origins remains to be determined.

MSCs cultured under hypoxic conditions have several advantages. Yu et al. reported that bone marrow-derived MSCs grown under 1% oxygen promoted liver regeneration and highly expressed VEGF in mice subjected to radical hepatectomies [21]. Zhao et al. reported that MSCs cultured in 1% oxygen maintained stemness in umbilical cord blood-derived CD34 + cells in part by increasing VEGF secretion and decreasing IL-6 secretion [22]. Wobma et al. reported that dual IFN- γ /hypoxia priming in MSCs induced greater immunosuppressive protein (IDO and HLA-G) upregulation than IFN- γ priming alone. Wobma et al. also performed proteome and

metabolome analyses on dual IFN- γ /hypoxia-primed MSCs. IFN- γ upregulated the expression of anti-pathogenic proteins, induced MSCs to limit inflammation and fibrosis, and promoted their survival. Hypoxia induced the cells to adapt to low oxygen via the upregulation of proteins involved in anaerobic metabolism, autophagy, angiogenesis, and cell migration [23]. Ho et al. reported that hypoxic preconditioning via spheroid formation accelerated segmental bone defect repair. MSCs in which hypoxia was induced via spheroid formation had higher cell viability, proangiogenic potential, and bone repair efficacy than normoxic MSCs [24].

The present and previous reports indicated that most MSCs were trapped in the lungs and did not migrate to the liver for 7 d after injection. MSC migration is a very important consideration when elucidating the therapeutic effects of MSCs. Certain reports underscored the importance of using conditioned medium or secreted exosomes. Lee et al. reported that human adipose-derived MSCs cultured in hypoxic media promoted mouse liver regeneration after a partial hepatectomy and expressed IL-6, TNF- α , HGF, and VEGF, all of which are important for liver regeneration [25]. Gonzalez-King et al. reported that HIF-1 α -overexpressing MSC-derived exosomes stimulated the Notch pathway and promoted angiogenesis [26]. The roles of trophic factors under different culture conditions, including exosomes, require further investigation.

5. Conclusions

A limitation of this study is that we could not use both hypoMSCs and normMSCs from the same donor, because each of these cells was prepared before use. In addition, short-term hypoxia exposure may have both inhibitory and stimulatory effects. Therefore, we used bone marrow-derived MSCs at the same passages, but originating from different sources.

MSCs have many benefits and advantages in cytotераpy. They can be obtained from medical waste, expand easily, can be preconditioned under hypoxia and with specific stimuli including IFN- γ , TNF- α , LPS, and IL-1 β , and can be applied on demand as allogeneic cells. A future research goal is the optimization of cell type, medium, exosomes, culture conditions, and disease targets in the development of MSC therapy.

Declarations

Availability of data and materials

The datasets produced and/or analysed during the current study are available from the corresponding author on reasonable request.

Competing interests

ST received research funding from NIHON PHARMACEUTICAL CO., LTD.

Ethics approval and consent to participate

Informed consent was obtained from each sample donor. All experiments were approved by the Ethics Committee of Niigata University, Niigata, Japan. All animal experiments were conducted in compliance with regulations and approved by the Institutional Animal Care and Committee at Niigata University.

Consent for publication

Not applicable.

Funding

This work was supported by NIHON PHARMACEUTICAL CO., LTD.

Author contributions

Conceived and designed the experiments: YK, AT, ST.
 Performed the experiments: YK, AT, JK, ML.
 Analyzed the data: YK, AT.
 Wrote the manuscript: YK, AT, ST.
 Obtained funding: AT, ST.
 Critical review of the manuscript: ST.

Acknowledgments

Not applicable.

Appendix A. Supplementary data

Supplementary data to this article can be found online at <https://doi.org/10.1016/j.reth.2019.08.005>.

References

- [1] Bernardi M, Caraceni P. Novel perspectives in the management of decompensated cirrhosis. *Nat Rev Gastroenterol Hepatol* 2018;15:753–64.
- [2] Feld JJ, Jacobson IM, Hézode C, Asselah T, Ruane PJ, Gruener N, et al. Sofosbuvir and velpatasvir for HCV Genotype 1, 2, 4, 5, and 6 infection. *N Engl J Med* 2015;373:2599–607.
- [3] Curry MP, O'Leary JG, Bzowej N, Muir AJ, Korenblat KM, Fenkel JM, et al. Sofosbuvir and velpatasvir for HCV in patients with decompensated cirrhosis. *N Engl J Med* 2015;373:2618–28.
- [4] Dienstag JL, Goldin RD, Heathcote EJ, Hann HW, Woessner M, Stephenson SL, et al. Histological outcome during long-term lamivudine therapy. *Gastroenterology* 2003;124:105–17.
- [5] Terai S, Tsuchiya A. Status of and candidates for cell therapy in liver cirrhosis: overcoming the “point of no return” in advanced liver cirrhosis. *J Gastroenterol* 2017;52:129–40.
- [6] Peng L, Xie DY, Lin BL, Liu J, Zhu HP, Xie C, et al. Autologous bone marrow mesenchymal stem cell transplantation in liver failure patients caused by hepatitis B: short-term and long-term outcomes. *Hepatology* 2011;54:820–8.
- [7] Suk KT, Yoon JH, Kim MY, Kim CW, Kim JK, Park H, et al. Transplantation with autologous bone marrow-derived mesenchymal stem cells for alcoholic cirrhosis: phase 2 trial. *Hepatology* 2016;64:2185–97.
- [8] Watanabe Y, Tsuchiya A, Seino S, Kawata Y, Kojima Y, Ikarashi S, et al. Mesenchymal stem cells and induced bone marrow-derived macrophages synergistically improve liver fibrosis in mice. *Stem Cells Transl Med* 2019;8:271–84.
- [9] Tsuchiya A, Kojima Y, Ikarashi S, Seino S, Watanabe Y, Kawata Y, et al. Clinical trials using mesenchymal stem cells in liver diseases and inflammatory bowel diseases. *Inflamm Regen* 2017;37:16.
- [10] Lin T, Pajarinen J, Nabeshima A, Lu L, Nathan K, Jamsen E, et al. Preconditioning of murine mesenchymal stem cells synergistically enhanced immunomodulation and osteogenesis. *Stem Cell Res Ther* 2017;8:277.
- [11] Shin S, Choi JW, Lim S, Lee S, Jun EY, Sun HM, et al. Anti-apoptotic effects of adipose-derived adherent stromal cells in mesenchymal stem cells exposed to oxidative stress. *Cell Biochem Funct* 2018;36:263–72.
- [12] Chan YC, Banerjee J, Choi SY, Sen CK. miR-210: the master hypoxamir. *Microcirculation* 2012;19:215–23.
- [13] Philipp D, Suhr L, Wahlers T, Choi YH, Paunel-Gorgulu A. Preconditioning of bone marrow-derived mesenchymal stem cells highly strengthens their potential to promote IL-6-dependent M2b polarization. *Stem Cell Res Ther* 2018;9:286.
- [14] Wang Y, Liu J, Jiang Q, Deng J, Xu F, Chen X, et al. Human adipose-derived mesenchymal stem cell-secreted CXCL1 and CXCL8 facilitate breast tumor growth by promoting angiogenesis. *Stem Cells* 2017;35:2060–70.
- [15] Sherman SE, Kuljanin M, Cooper TT, Putman DM, Lajoie GA, Hess DA. High aldehyde dehydrogenase activity identifies a subset of human mesenchymal stromal cells with vascular regenerative potential. *Stem Cells* 2017;35:1542–53.
- [16] Elabd C, Ichim TE, Miller K, Anneling A, Grinstein V, Vargas V, et al. Comparing atmospheric and hypoxic cultured mesenchymal stem cell transcriptome: implication for stem cell therapies targeting intervertebral discs. *J Transl Med* 2018;16:222.
- [17] Buravkova LB, Andreeva ER, Gogvadze V, Zhivotovsky B. Mesenchymal stem cells and hypoxia: where are we? *Mitochondrion* 2014;19(Pt A):105–12.
- [18] Gao S, Xiang C, Qin K, Sun C. Mathematical modeling reveals the role of hypoxia in the promotion of human mesenchymal stem cell long-term expansion. *Stem Cell Int* 2018;2018:9283432.
- [19] Vertelov G, Kharazi L, Muralidhar MG, Sanati G, Tankovich T, Kharazi A. High targeted migration of human mesenchymal stem cells grown in hypoxia is associated with enhanced activation of RhoA. *Stem Cell Res Ther* 2013;4:5.
- [20] Yu Y, Yin Y, Wu RX, He XT, Zhang XY, Chen FM. Hypoxia and low-dose inflammatory stimulus synergistically enhance bone marrow mesenchymal stem cell migration. *Cell Prolif* 2017;50.
- [21] Yu J, Yin S, Zhang W, Gao F, Liu Y, Chen Z, et al. Hypoxia preconditioned bone marrow mesenchymal stem cells promote liver regeneration in a rat massive hepatectomy model. *Stem Cell Res Ther* 2013;4:83.
- [22] Zhao D, Liu L, Chen Q, Wang F, Li Q, Zeng Q, et al. Hypoxia with Wharton's jelly mesenchymal stem cell coculture maintains stemness of umbilical cord blood-derived CD34⁺ cells. *Stem Cell Res Ther* 2018;9:158.
- [23] Wobma HM, Tamargo MA, Goeta S, Brown LM, Duran-Struock R, Vunjak-Novakovic G. The influence of hypoxia and IFN-gamma on the proteome and metabolome of therapeutic mesenchymal stem cells. *Biomaterials* 2018;167:226–34.
- [24] Ho SS, Hung BP, Heyrani N, Lee MA, Leach JK. Hypoxic preconditioning of mesenchymal stem cells with subsequent spheroid formation accelerates repair of segmental bone defects. *Stem Cells* 2018;36:1393–403.
- [25] Lee SC, Jeong HJ, Lee SK, Kim SJ. Hypoxic conditioned medium from human adipose-derived stem cells promotes mouse liver regeneration through JAK/STAT3 signaling. *Stem Cells Transl Med* 2016;5:816–25.
- [26] Gonzalez-King H, García NA, Ontoria-Oviedo I, Ciria M, Montero JA, Sepulveda P. Hypoxia inducible factor-1alpha potentiates jagged 1-mediated angiogenesis by mesenchymal stem cell-derived exosomes. *Stem Cells* 2017;35:1747–59.